Overlapping-image multimode interference couplers with a reduced number of self-images for uniform and nonuniform power splitting

M. Bachmann, P. A. Besse, and H. Melchior

Overlapping-image multimode interference (MMI) couplers, a new class of devices, permit uniform and nonuniform power splitting. A theoretical description directly relates coupler geometry to image intensities, positions, and phases. Among many possibilities of nonuniform power splitting, examples of 1×2 couplers with ratios of 15:85 and 28:72 are given. An analysis of uniform power splitters includes the well-known $2 \times N$ and $1 \times N$ MMI couplers. Applications of MMI couplers include mode filters, mode splitters–combiners, and mode converters.

Key words: Integrated optics, optical splitters and combiners, multimode interference, Talbot effect.

1. Introduction

Since the first suggestion by Bryngdahl[1] to achieve self-imaging in uniform-slab waveguides, there has been a growing interest in the application of multimode interference (MMI) effects for the splitting and combining of multiple optical beams.[2] Because of their excellent properties and ease of fabrication, MMI couplers have been incorporated into more complex photonic integrated circuits, such as ring lasers,[3] polarization-insensitive Mach–Zehnder interferometer (MZI) switches,[4–6] optical hybrids for phase diversity networks,[7,8] and polarization diversity receivers.[9] A more detailed overview on realized MMI couplers is given in Ref. 2.

The self-imaging phenomena has theoretically been described for general $N \times N$ MMI couplers that form N-fold images at a length of $3L_c/N$, where L_c is the coupling length between the two lowest order modes.[10] Analytical expressions for positions and phases of the N-fold images have been given. Phases of self-images are of practical importance for components that work with optical interferences such as generalized MZI switches[6,11] and wavelength division multiplexers.[12]

The authors are with the Institute of Quantum Electronics, Swiss Federal Institute of Technology, CH-8093 Zurich, Switzerland.

Received 7 November 1994; revised manuscript received 1 May 1995.

0003-6935/95/306898-13$06.00/0.

In addition to these $N \times N$ MMI couplers based on general interference, two types of MMI couplers based on restricted interference, called paired and symmetric interference,[2] have been identified for symmetric input light distributions. Paired interference is obtained for input light distributions that do not excite modes of numbers 2, 5, 8, . . . of the MMI section.[13,14] The resulting $2 \times N$ MMI couplers form N-fold self-images at reduced lengths of L_c/N. Symmetric interference is obtained with excitation of only symmetric modes of the MMI coupler.[15,16] The N-fold images are formed at $3L_c/4N$ in these $1 \times N$ MMI devices. MMI couplers based on restricted interference are of importance because of their reduced length. Nevertheless, image formation including phases has yet to be derived.

In this paper the general theory of $N \times N$ MMI couplers[10] is applied to the special cases of $2 \times N$ and $1 \times N$ MMI couplers operating with restricted interference. Input light distributions are symmetrical and positioned at $W/3$ or $W/2$, where W is the width of the MMI coupler. At the output of the MMI coupler, overlapping images are obtained. Phases and intensities of the images are derived by calculation of the interference. Nonvanishing images have equal intensity, and uniform power splitting is confirmed. Phases of the images, as given in Ref. 17 without explanation, are derived here. The results are written in a compact form, ready for use in generalized MZI switches[6,11] and in wavelength division multiplexer devices.[12] Furthermore, the derivation is performed in a more general way to include all

the overlapping-image MMI couplers. To our knowledge, a complete theoretical description of these couplers is presented for the first time. Intensities, positions and phases of the self-images are given in all cases.

Imaging properties of antisymmetric distributions are discussed as well. Based on the different imaging properties of symmetric and antisymmetric light distributions, MMI couplers with useful functionalities such as mode filters, mode splitters, mode combiners, and mode convertors are proposed. Such devices can be used to improve the on–off ratio in MZI modulators or to overlap and separate the pump and probe signals in all optical switches.[18]

In general, overlapping-image MMI couplers produce self-images with different intensities. We identify nonuniform 1×2 power splitters with splitting ratios of 15:85 or 28:72. These can be used in fiber-optic networks to perform the tap function, which requires only a small part of the light to be extracted from an optical channel. Another application is in ring lasers in which the splitting ratio of the coupler influences the characteristics of the entire device.[19] In addition, asymmetric splitting ratios are advantageous in the couplers of MZI devices when losses or gain are involved.[20] Here, beside the case of 1×2 splitters, nonuniform power splitting in overlapping-image MMI couplers is analyzed in general. All the different possible discrete splitting ratios are treated and examples are presented. Applications are not yet obvious but may show up in the future. The same holds for the generalized phase diversity relation in $N \times N$ MMI couplers, which is given for overlapping images obtained by the simultaneous excitation of two input channels.

2. Problem Definition for Overlapping Images

MMI couplers are widely used in guided wave optics. In general, light of one input channel is distributed to one or more output channels. Figure 1 schematically shows a 4×4 MMI coupler including the x, y, and z axes as chosen in this paper. The three-dimensional problem is reduced to two dimensions by the use of the effective index method. The MMI coupler is therefore defined by its length L, its width W, and its (effective) refractive index n at operating wavelength λ.

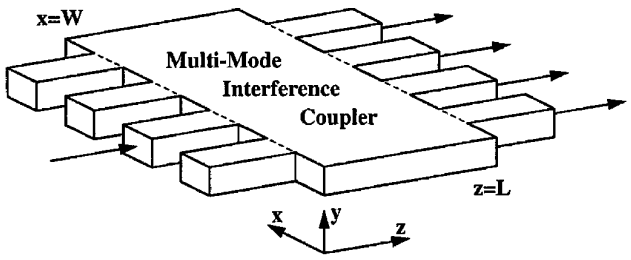

Fig. 1. Schematic view of a $N \times N$ MMI coupler ($N = 4$). Light from the input waveguide is launched into the MMI section, propagated, and imaged into the output waveguides.

We have already reported an analytical theory giving the positions, amplitudes, and phases of the self-images in $N \times N$ MMI couplers[10]: N self-images of equal intensities $1/N$ are formed at the output of MMI couplers of length

$$L_N^M = \frac{M}{N} 3L_c, \tag{1}$$

where M and N are any positive integers without common divisor and where L_c is the coupling length between the two lowest order modes. With strongly guided eigenmodes E_i in the MMI section and paraxial approximation for the propagation constants β_i, L_c can be written as[10]

$$L_c \cong \frac{4nW^2}{3\lambda}. \tag{2}$$

In short MMI couplers with $M = 1$ images are positioned as shown in Fig. 2. Note the additional free parameter a limited to $0 \le a \le W/N$ for the input and output positions. The phases ($\varphi = \omega t - kz$) for imaging input i to output j have been given in a compact form.[10] This description of the imaging phenomena is well suited for separated input and output channels. However, if free parameter a approaches one of its limits, previously separated self-images overlap and cause interference. The overlapping images form a new light distribution. Complete interference between one upright and one inverted image mirrored with respect to the propagation axis (see Fig. 2) is obtained only for purely symmetric or purely antisymmetric optical field distributions at the input of the MMI coupler. These configurations, called overlapping-image MMI couplers, are analyzed. Because previously separated images merge in pairs, a reduced number of images is obtained. We strictly distinguish between the number N of images in conventional $N \times N$ couplers of length L_N^M and the reduced number K of images in order to avoid confusion.

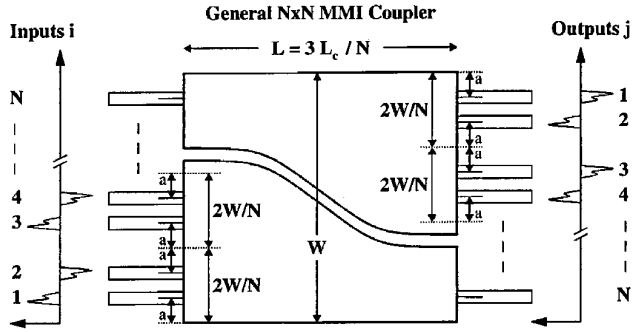

Fig. 2. General $N \times N$ MMI coupler with access waveguides for arbitrary N. Note the existence of upright and mirrored images. Parameter a can be chosen freely between $0 \le a \le W/N$. At its limits of $a = 0$ or $a = W/N$, images merge in pairs. An overlapping-image MMI coupler is formed.

3. Self-Imaging Properties of Overlapping-Image Multimode Inference Couplers

A reduced number of images at the output of MMI couplers is obtained for selected input positions. For $M = 1$ these positions are obtained when free parameter a is chosen as defined in Fig. 2 at one of its limits. The merging of two output channels in this configuration could be considered by the calculation of the interference taking place between the two images. In order to derive equations for general M, however, we use the concept of the extended MMI coupler as introduced in Ref. 10. Positions, intensities, and phases of the reduced number of images resulting from interference in the overlapping-image MMI couplers are calculated for purely symmetric and purely antisymmetric input distributions. Arbitrary light distributions can be analyzed as a superposition.

A. Interfering Images: Intensities and Phases

Interference between two equal light distributions of intensity $1/N$ occurs at the output of the MMI coupler. For two interfering images with known phases φ_1 and φ_2, intensity r^2 and phase Φ of the resulting image are derived from the addition of the complex amplitudes:

$$r \exp(j\Phi) = \frac{1}{\sqrt{N}} \exp(j\varphi_1) + \frac{1}{\sqrt{N}} \exp(j\varphi_2). \tag{3}$$

With definition of phase difference $\Delta\varphi = \varphi_1 - \varphi_2$ and mean phase $\overline{\varphi} = (\varphi_1 + \varphi_2)/2$, we obtain

$$r \exp(j\Phi) = \frac{2}{\sqrt{N}} \cos\left(\frac{\Delta\varphi}{2}\right) \exp(j\overline{\varphi}). \tag{4}$$

A comparison of the magnitude and phase yields

$$r^2 = \frac{4}{N} \cos^2\left(\frac{\Delta\varphi}{2}\right),$$

$$\Phi = \begin{cases} \overline{\varphi} & \text{for } \cos\left(\dfrac{\Delta\varphi}{2}\right) > 0 \\ \overline{\varphi} + \pi & \text{for } \cos\left(\dfrac{\Delta\varphi}{2}\right) < 0. \end{cases} \tag{5}$$

This general formula for interfering two equally intense images is now applied to the interference taking place at the output of the overlapping-image MMI coupler.

B. Extended Multimode Inference Coupler

The concept of the extended MMI coupler[10] is used for mathematical simplicity and to cover the case for general M and N. The extended MMI coupler consists of a virtual MMI section added to the real MMI coupler (Fig. 3). Input light distribution and eigenmodes of the MMI coupler are extended to form antisymmetrical functions, which then are periodically extended to the whole x axes. Therefore each point on the x axes has its correspondent in the real MMI section caused by the $2W$ periodicity and the antisymmetricity.

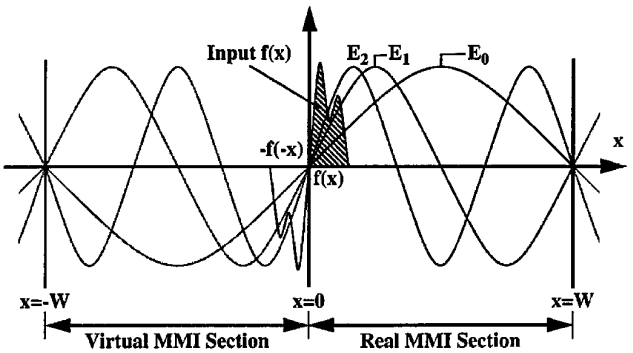

Fig. 3. MMI section with input light distribution $f(x)$ and eigenmodes $E_i(x)$ of the structure. Functions $E_i(x)$ and $f(x)$ are antisymmetrically extended to a virtual MMI section and periodically repeated on the whole x axes.

The formation of the self-images in the extended MMI coupler is based on the strong guiding approximation and the paraxial approximation. The light distribution, $f_{\text{out}}(x)$, at the output of the MMI coupler of length $L_N{}^M$ is illustrated in Fig. 4 and is given as[10]

$$f_{\text{out}}(x) = \frac{1}{C} \sum_{q=0}^{N-1} f_{\text{in}}(x - x_q) \exp(j\varphi_q), \tag{6}$$

a sum of N equally intense images numbered by $q = 0, 1, \ldots, N-1$. Positions x_q and relative phases φ_q of images q are

$$x_q = (2q - N) \frac{M}{N} W, \tag{7}$$

$$\varphi_q = q(N - q) \frac{M}{N} \pi. \tag{8}$$

Here $f_{\text{in}}(x)$ is the antisymmetrically extended input light distribution with $2W$ periodicity, and C is the complex normalization constant explicitly given in Ref. 10. It can be written as

$$C = \exp\left(j \frac{2\pi n}{\lambda} L_N{}^M\right) \sum_{q=0}^{N-1} \exp\left[j\pi \frac{M}{N} q(N - q)\right]. \tag{9}$$

Its magnitude is $|C| = \sqrt{N}$. For $M = 1$ it is

$$C = \sqrt{N} \exp(-j\varphi_0),$$

$$\varphi_0 = -\frac{2\pi n}{\lambda} L_N{}^{M=1} - \frac{\pi}{4}(N - 1). \tag{10}$$

Absolute phases are obtained by the addition of the constant phase, φ_0, and the relative phases, φ_q, of the images.

Another approach to understanding the $N \times N$ MMI couplers is based on the Talbot effect.[21,22] The periodically repeated input distribution in Fig. 3

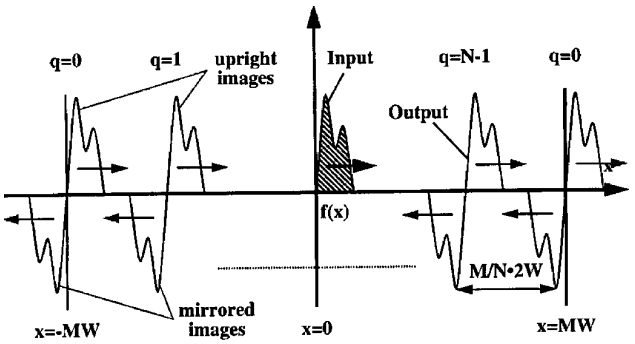

Fig. 4. Self-images formed at the output of a MMI coupler of length L_N^M in the extended MMI coupler. Half of the images are upright and half of them are mirrored. For input shifting along the arrow, outputs are shifted according to the arrows also. For input positions in which upright and mirrored images interfere, overlapping-image MMI couplers are obtained.

forms two separated (Talbot) arrays with $2W$ periodicity. Selected input positions lead to coherent overlap between upright and mirrored Talbot images. This is the basis of the overlapping-image MMI couplers discussed here.

C. Overlapping Images

Overlapping images are obtained as follows. Shifting input light distribution $f(x)$ in the extended MMI coupler along the x axes (see Fig. 4) moves the upright images in the same direction and the mirrored images in the opposite direction. Upright and mirrored images cross for the input positions

$$x_i^{\text{in}} = i\,\frac{M}{N}\,W, \qquad \text{with integer } i. \tag{11}$$

Interference takes place between upright images q and mirrored images $q + i$. Complete interference is obtained for either symmetrical or antisymmetrical input light distributions. The number of self-images is reduced because two images interfere into one. Output images are numbered with indices $j = 2N - 2q - i$ and are formed at the positions

$$x_j^{\text{out}} = x_q + x_i^{\text{in}} = MW - j\,\frac{M}{N}\,W, \qquad \text{with even } i + j. \tag{12}$$

The phases of the two interfering images are

$$\begin{aligned} \varphi_1 &= \varphi_q, \\ \varphi_2 &= \varphi_{q+i} + b\pi, \end{aligned} \tag{13}$$

where b takes the phase shift caused by mirroring of the second image into account:

$$\begin{aligned} b &= 1, \qquad \text{symmetrical input,} \\ b &= 0, \qquad \text{antisymmetrical input.} \end{aligned} \tag{14}$$

With Eq. (8) introduced into Eq. (13), the phase differences and mean phases of resulting images j are

$$\begin{aligned} \Delta\varphi_{ij} &= \varphi_1 - \varphi_2 = (N - j)i\,\frac{M}{N}\,\pi - b\pi, \\ \overline{\varphi_{ij}} &= \frac{\varphi_1 + \varphi_2}{2} = -(i^2 + j^2)\,\frac{M}{N}\,\frac{\pi}{4} + jM\,\frac{\pi}{2} + \frac{b\pi}{2}\cdot \end{aligned} \tag{15}$$

Intensities r_{ij}^2 and phases Φ_{ij} of the images are obtained by introduction into Eq. (5):

$$r_{ij}^2 = \frac{4}{N}\cos^2\left[(N - j)i\,\frac{M}{N}\,\frac{\pi}{2} - b\,\frac{\pi}{2}\right],$$

$$\Phi_{ij} = \begin{cases} -(i^2 + j^2)\,\dfrac{M}{N}\,\dfrac{\pi}{4} + jM\,\dfrac{\pi}{2} + \dfrac{b\pi}{2} \\ \quad \text{for } \cos\left[(N - j)i\,\dfrac{M}{N}\,\dfrac{\pi}{2} - b\,\dfrac{\pi}{2}\right] > 0 \\ -(i^2 + j^2)\,\dfrac{M}{N}\,\dfrac{\pi}{4} + jM\,\dfrac{\pi}{2} + \dfrac{b\pi}{2} + \pi \\ \quad \text{for } \cos\left[(N - j)i\,\dfrac{M}{N}\,\dfrac{\pi}{2} - b\,\dfrac{\pi}{2}\right] < 0. \end{cases} \tag{16}$$

Images do not have equal intensities anymore.

4. Uniform Power Splitters

The self-images in overlapping-image MMI couplers are formed at the output positions, x_j^{out}, for light input at the specially selected positions, x_i^{in}. Here all the possible configurations with uniform power splitting are identified and discussed. Image positions and phases, which are of practical importance, are given in a compact form.

A. Possible Input Positions

Uniform power splitting is obtained if intensities r_{ij}^2 of Eq. (16) are zero or constant for all allowed images with even $i + j$. For a fixed input channel i, the arguments of the cosine square in Eq. (16) for two adjacent output images are spaced by

$$s = i\,\frac{M}{N}\,\pi = x_i^{\text{in}}\,\frac{\pi}{W}\cdot \tag{17}$$

The illustration of the cosine-square function in Fig. 5 shows that constant intensities are possible only if $s = Z\pi/2$ or $s = Z\pi/3$ for integer Z. With Eq. (17) this restriction on spacing s can be written as a restriction on the possible input positions:

$$x_i^{\text{in}} = Z\,\frac{W}{2} \qquad \text{or } x_i^{\text{in}} = Z\,\frac{W}{3}\cdot \tag{18}$$

These input positions correspond in the real MMI section to the edges, the center, and one or two thirds of the MMI coupler. Input positioned at the edges is not considered here because light distributions would extend out of the real MMI section. It will become clear, however, that antisymmetrical distributions

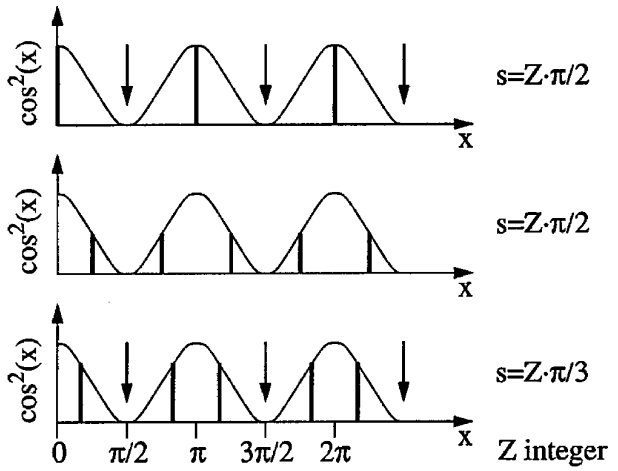

Fig. 5. Illustration of possible values of spacing s, permitting equally intense output images in overlapping-image MMI couplers. Arrows mark the channels with zero intensity, and vertical lines represent channels with constant light intensity.

can form images at the edges. Below, inputs at the center and at one third of the MMI coupler are considered in detail. All other input positions of overlapping-image MMI couplers yield nonuniform splitting ratios.

B. Input at the Center of the Multimode Interference Coupler

With $x^{\text{in}} = ZW/2$, input is at the center or at corresponding positions in the extended MMI coupler for Z odd. As we can see from Eq. (11), for integer i, N has to be even and Z has to be a multiple of M, because M and N have no common divisor. With $Z = MZ'$, Z' is odd when Z is odd. We have

$$i = \frac{Z}{M}\frac{N}{2} = Z'\frac{N}{2} = \frac{N}{2}. \tag{19}$$

All the odd Z' describe the same physical configuration, with numbering index $q + i$ of the mirrored images replaced by $q + i \pm N, q + i \pm 2N, \ldots$. In Eq. (19) we therefore have set $Z' = 1$. Input is positioned in the extended MMI coupler at

$$x^{\text{in}} = M\frac{W}{2}, \tag{20}$$

which corresponds in the real MMI section to input at the center $x^{\text{in}} = W/2$, because M is odd. Output images in the extended MMI coupler are obtained with Eq. (12) at

$$x_j^{\text{out}} = MW - j\frac{M}{N}W \qquad \text{for } j + \frac{N}{2} \text{ even}. \tag{21}$$

From Eq. (16) we obtain the intensities and phases of the images with $i = N/2$. Because the argument of the cosine square is a multiple of $\pi/4$ we can write

$$r_j^2 = \begin{cases} 4/N & \text{for } M(N - j) - 2b = 4k \\ 2/N & \text{for } M(N - j) - 2b = 4k \pm 1 \\ 0 & \text{for } M(N - j) - 2b = 4k + 2 \end{cases},$$

$$\Phi_j = \begin{cases} -NM\dfrac{\pi}{16} - j^2\dfrac{M}{N}\dfrac{\pi}{4} + jM\dfrac{\pi}{2} + \dfrac{b\pi}{2} \\ \quad \text{for } M(N - j) - 2b = 8k,\ 8k \pm 1 \\ -NM\dfrac{\pi}{16} - j^2\dfrac{M}{N}\dfrac{\pi}{4} + jM\dfrac{\pi}{2} + \dfrac{b\pi}{2} + \pi \\ \quad \text{for } M(N - j) - 2b = \text{otherwise}. \end{cases} \tag{22}$$

Here k is any integer number. In a further discussion we distinguish between the two cases of N as an odd and an even multiple of 2.

1. N = 2K *with odd* K

Output images are obtained for even $j + N/2 = j + K$, and therefore for odd j. Because here $M(N - j) - 2b$ is odd in Eq. (22), we obtain for all images equal intensities:

$$r_j^2 = \frac{2}{N} = \frac{1}{K}. \tag{23}$$

The number of self-images in the extended MMI coupler is $N = 2K$, yielding K images in the real MMI section. This is valid for symmetrical as well as antisymmetrical input light distributions. The phases of the images as calculated from Eq. (22) are

$$\Phi_j = \begin{cases} -j^2\dfrac{M}{K}\dfrac{\pi}{8} + jM\dfrac{\pi}{2} - MK\dfrac{\pi}{8} + \dfrac{b\pi}{2} \\ \quad \text{for} \quad M(2K - j) - 2b = 8k \pm 1,\ k \text{ integer} \\ -j^2\dfrac{M}{K}\dfrac{\pi}{8} + jM\dfrac{\pi}{2} - MK\dfrac{\pi}{8} + \dfrac{b\pi}{2} + \pi \\ \quad \text{for} \quad M(2K - j) - 2b = \text{otherwise}. \end{cases} \tag{24}$$

Phases are different for symmetrical and antisymmetrical inputs by a phase difference of $\pm\pi/2$. Even as symmetrical and antisymmetrical inputs produce self-images at the same positions, general light distributions do not build self-images because of these phase differences. In the case of $K = 1$, for example, one image with a phase shift of $\pi/2$ introduced between symmetrical and antisymmetrical light distributions is obtained.

2. N = 4K

For even $j + N/2 = j + 2K$, j and therefore $M(N - j) - 2b$ have to be even. With Eq. (22), we

obtain for the intensities

$$r_j^2 = \begin{cases} 4/N = 1/K & \text{for } M\left(2K - \frac{j}{2}\right) - b \text{ even} \\ 0 & \text{for } M\left(2K - \frac{j}{2}\right) - b \text{ odd.} \end{cases} \quad (25)$$

Every second image of even j has zero intensity. Nonvanishing images have different positions for symmetrical and antisymmetrical light distributions, which permits mode splitting. It is described in more detail below.

Phases of the nonvanishing images are with Eq. (22):

$$\Phi_j = \begin{cases} -KM\frac{\pi}{4} - j^2\frac{M}{K}\frac{\pi}{16} + jM\frac{\pi}{2} + b\frac{\pi}{2} \\ \qquad \text{for } M\left(K - \frac{j}{4}\right) - \frac{b}{2} \text{ even} \\ -KM\frac{\pi}{4} - j^2\frac{M}{K}\frac{\pi}{16} + jM\frac{\pi}{2} + b\frac{\pi}{2} + \pi \\ \qquad \text{for } M\left(K - \frac{j}{4}\right) - \frac{b}{2} \text{ odd,} \end{cases} \quad (26)$$

which can be simplified to

$$\Phi_j = 3MK\frac{\pi}{4} - j^2\frac{M}{K}\frac{\pi}{16} + jM\frac{\pi}{4}. \quad (27)$$

In the extended MMI coupler we have $N/2 = 2K$ images and therefore K images in the real MMI coupler.

3. General Result

We consider an MMI coupler of arbitrary length with input at the center. Input light distribution is a superposition of a symmetrical and an antisymmetrical part. These two parts are discussed separately (Fig. 6). At the device length of

$$L_K^M = \frac{M}{K}\frac{3}{4}L_c, \quad (28)$$

where M and K are any integers without common divisor, K images with equal intensities are formed. To proof it, we consider the cases for M odd, M as an odd multiple of 2, and M as a multiple of 4 separately.

1. For odd M and for M having no common divisor with K, $N = 4K$ and M have no common divisor. This is the above case 2 with K images.
2. For M being an odd multiple of 2 and having no common divisor with K, K must be odd. With $N = 2K$ and $M' = M/2$ having no common divisor, we obtain the above case 1 with K images again.
3. If M is a multiple of 4, $M = 4M'$, we have a device of length $L = (M'/K)3L_c$. Because K has to be odd, we do not have the case of a reduced number of images. Note that M' and K have no common divisor and that we have K images.

We have theoretically derived that an either symmetrical or antisymmetrical input at the center of an MMI coupler of length L_K^M yields K images of equal intensities. In addition, phases and positions have been given. Note that the length of the MMI coupler is only one fourth of the length of the conventional

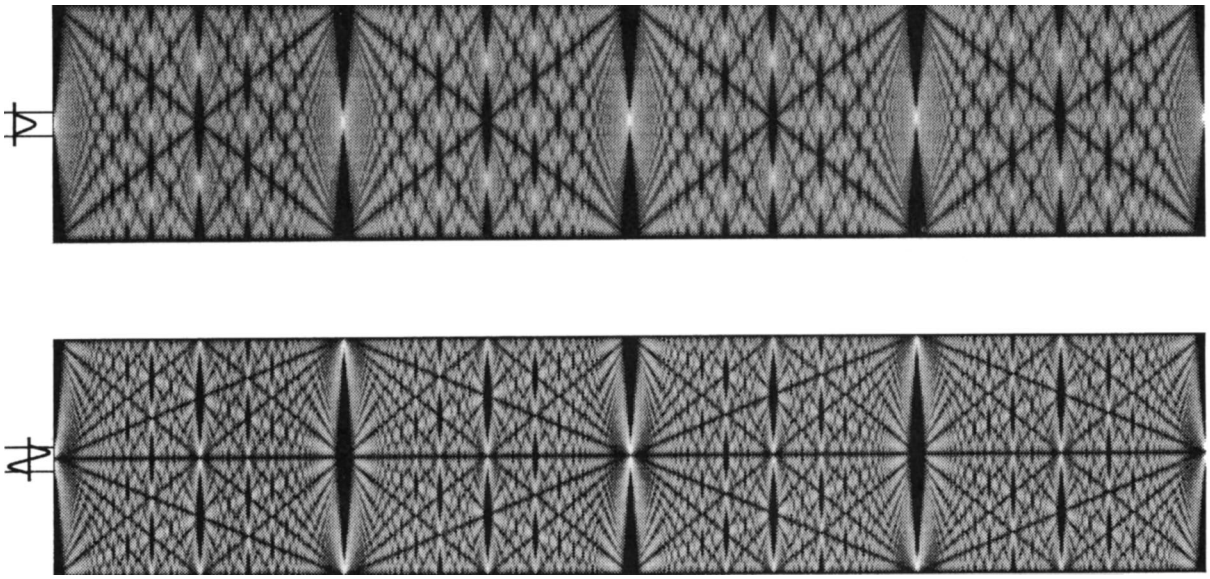

Fig. 6. Image formation for light input at the center of the MMI coupler. The upper section shows imaging of symmetrical input and the lower section shows that of antisymmetrical input, respectively. The whole length of the MMI coupler is one imaging length, $3L_c$. Note that for both input configurations K images are obtained at $L = (3M/4K)L_c$ for any integer K and M without common divisor. Image positions, however, differ for symmetrical and antisymmetrical inputs. This allows for mode filtering or mode splitting.

device as defined in Eq. (1). Remember that arbitrary input distributions do not form self-images at the reduced length. Nevertheless the device is useful in integrated optics, in which light distributions in waveguides most often are symmetrical.

C. Input at One Third of the Multimode Interference Coupler

The second configuration of the overlapping-image MMI couplers with equally intense images has light input at one third. Input at one or two thirds or at corresponding positions in the extended MMI coupler is obtained for $x^{\text{in}} = ZW/3$, with Z no multiple of 3. For integer i, N must be a multiple of 3 and Z a multiple of M [see Eq. (11)]. With $Z = MZ'$ and $N = 3K$ we have

$$i = \frac{Z}{M}\frac{N}{3} = Z'\frac{N}{3} = 2\frac{N}{3} = 2K. \tag{29}$$

Because Z is not a multiple of 3, neither is Z'. The remaining Z' describe the same physical configuration, because inputs at one and two thirds of the MMI coupler are symmetric problems. For mathematical simplicity we have set $Z' = 2$. Light input in the extended MMI coupler is at

$$x^{\text{in}} = M\frac{2W}{3}, \tag{30}$$

which corresponds to input at one or two thirds in the real MMI section. Output images are with Eq. (12) at

$$x_j^{\text{out}} = MW - \frac{j}{3}\frac{M}{K}W, \qquad \text{with } j \text{ even}. \tag{31}$$

Introduction into Eq. (16) yields intensities r_j^2 of the images. It can be seen that uniform power splitting is not possible for $b = 0$. This means that antisymmetrical input distributions at one or two thirds of the MMI coupler do not produce equally intense images at reduced lengths. Symmetrical input with $b = 1$ yields the intensities of the images

$$r_j^2 = \begin{cases} 0 & \text{for } j = 6k \\ 1/K & \text{for } j = 6k \pm 2, \end{cases} \tag{32}$$

where k is any integer. The number of self-images in the extended MMI coupler is $2N/3 = 2K$, yielding K images in the real MMI section. The phases of the nonvanishing images with symmetrical input are with Eq. (16):

$$\Phi_j = \begin{cases} -KM\dfrac{\pi}{3} - j^2\dfrac{M}{K}\dfrac{\pi}{12} + jM\dfrac{\pi}{2} + \dfrac{\pi}{2} \\ \quad \text{for } M(3K - j) = 6k + 1,\ 6k + 2 \\ -KM\dfrac{\pi}{3} - j^2\dfrac{M}{K}\dfrac{\pi}{12} + jM\dfrac{\pi}{2} + \dfrac{\pi}{2} + \pi \\ \quad \text{for } M(3K - j) = 6k - 1,\ 6k - 2. \end{cases} \tag{33}$$

Symmetrical input at one or two thirds of an MMI coupler of length

$$L_K^M = \frac{M}{K}L_c \tag{34}$$

therefore yields K images of equal intensities. This is valid for general M and K without common divisors. The complete theoretical derivation has been given here, to our knowledge, for the first time. Again, positions and phases of the images have been derived. An illustration is given in Fig. 7.

5. Application to Practical Multimode Interference Couplers with $M = 1$

In Section 3 we considered overlapping-image MMI couplers in general. All possible configurations for uniform power splitting were identified in Section 4. Here, above results for general M are used for the consideration of special cases of short practical devices with $M = 1$.

After a description of nonuniform power splitting for $M = 1$ in detail, the $1 \times K$ and $2 \times K$ uniform power splitters with input at the center and at one third of the MMI coupler are worked out explicitly. Devices based on the different imaging properties of symmetrical and antisymmetrical modes are then introduced. These include a mode filter, a mode splitter–combiner, and a mode converter. In addition, devices allowing for cosine-square intensity distributions are shown. Finally, an MMI coupler with $N = 12$ is described in order to round up the considerations. This MMI coupler includes the different cases of uniform $1 \times K$ and $2 \times K$ as well as nonuniform power splitting in one single device.

A. Nonuniform Power Splitting

Overlapping-image MMI couplers produce nonuniform power distributions. For MMI coupler of length as given in Eq. (1) with $M = 1$, overlapping images are obtained for the input positions of Eq. (11) at the output positions of Eq. (12), as illustrated in Fig 8:

$$x_i^{\text{in}} = i\frac{W}{N}, \qquad i = (0),\ 1,\ 2,\ 3,\ \ldots,\ N - 1,\ (N), \tag{35}$$

$$x_j^{\text{out}} = W - j\frac{W}{N},$$

$$j = (0),\ 1,\ 2,\ 3,\ \ldots,\ N - 1,\ (N), \text{ and } i + j \text{ even}. \tag{36}$$

The numbers in parentheses yield channels positioned at the edges of the MMI coupler, which is possible for antisymmetrical light distributions. Intensities and phases of the images are obtained

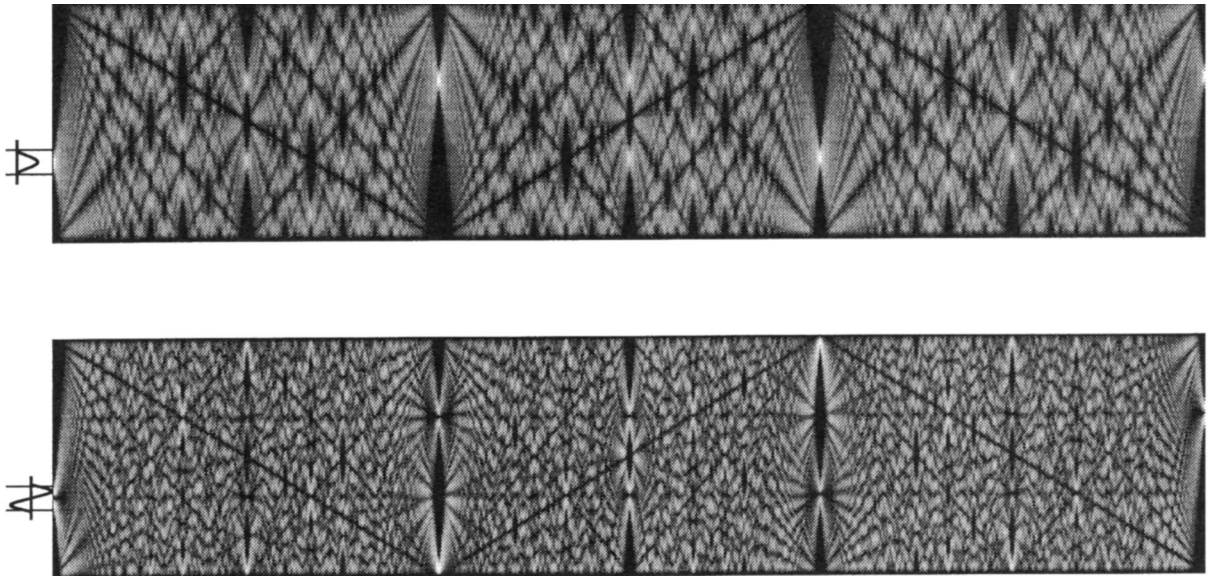

Fig. 7. Image formation for light input at one third of the MMI coupler. Only symmetrical light distributions (upper section) form a reduced number of equally intense self-images: K images at $L = (M/K)L_c$. Antisymmetrical light distributions (lower section) do not form equally intense self-images at a reduced length. The total device length is $3L_c$.

from Eq. (16) with $M = 1$:

$$r_{ij}^{\,2} = \frac{4}{N}\cos^2\left[(N - j)i\,\frac{\pi}{2N} - b\,\frac{\pi}{2}\right],$$

$$\Phi_{ij} = \begin{cases} -(i^2 + j^2)\,\dfrac{\pi}{4N} + j\,\dfrac{\pi}{2} + b\,\dfrac{\pi}{2} \\ \quad \text{for } \cos\left[(N - j)i\,\dfrac{\pi}{2N} - b\,\dfrac{\pi}{2}\right] > 0 \\ -(i^2 + j^2)\,\dfrac{\pi}{4N} + j\,\dfrac{\pi}{2} + b\,\dfrac{\pi}{2} + \pi \\ \quad \text{for } \cos\left[(N - j)i\,\dfrac{\pi}{2N} - b\,\dfrac{\pi}{2}\right] < 0. \end{cases} \tag{37}$$

For the absolute phases to be obtained, constant phase φ_0 of Eq. (10) must be added to these relative phases Φ_{ij}. Calculations can easily be done for any specific example. To give an impression of the possibilities, we look at the intensities of the images for symmetric inputs. For $N \le 12$ and all possible input positions x_i^{in} of overlapping-image MMI couplers, the splitting ratios are given in Table 1. Nonuniform power splitting into two channels is of the highest interest. From the table we find the possibilities

$$100{:}0,\ 85{:}15,\ 72{:}28,\ 50{:}50. \tag{38}$$

This covers the whole splitting range from 0 to 1 in steps. We have already reported on a variation of the rectangular devices: the butterfly MMI couplers.[23] Power splitting into two channels at arbitrary ratios has been obtained.

For antisymmetrical inputs the splitting ratios are not the same as for symmetrical input distributions. A separate table can easily be calculated. Note that images can be cut into parts at the edges of the MMI coupler (see Figs. 6 and 7).

B. Input at the Center: Uniform $1 \times K$ Multimode Interference Coupler

Positioning input light at the center of a MMI coupler permits uniform power splitting into K images at a reduced length, as was discussed in Subsection 4.B for general M. Short devices are obtained for $M = 1$ and $N = 4K$. We are interested in symmetrical light distributions and therefore set $b = 1$. A symmetrical input at the center only excites symmetrical eigenmodes of the MMI coupler. This picture has been used for the derivation of the image positions.[15]

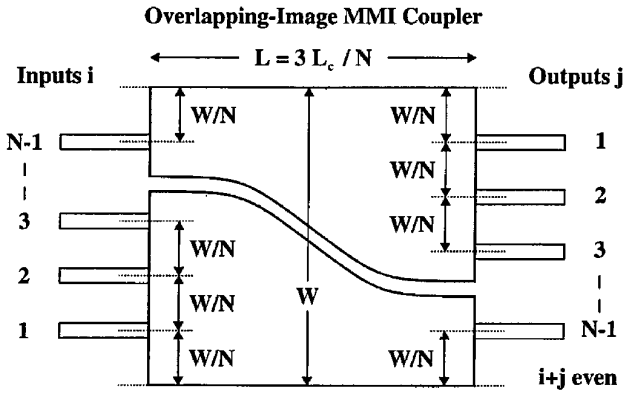

Fig. 8. Overlapping-image MMI couplers with a reduced number of self-images. For input channel i, output channels j with odd $i + j$ always have zero light intensities. The number of images is reduced. Intensities and phases of the remaining self-images are given in the text. Uniform as well as nonuniform power splitting is possible.

Table 1. Overlapping-Image MMI Couplers Permit Nonuniform Splitting Ratios[a]

Length ($L_N = 3L_c/N$)	Input Position ($x^{in} = iW/N$)	Intensity Distribution at Output (%)	
$N = 2$	$i = 1$	100	
$N = 3$	$i = 1, 2$	100	⇐
$N = 4$	$i = 1, 3$	85:15	⇐
	$i = 2$	100	
$N = 5$	$i = 1, \ldots, 4$	72:28	⇐
$N = 6$	$i = 1, 5$	62:33:5	
	$i = 2, 4$	50:50	⇐
	$i = 3$	33:33:33	
$N = 7$	$i = 1, \ldots, 6$	54:35:11	
$N = 8$	$i = 1, 3, 5, 7$	48:35:15:2	
	$i = 2, 6$	50:25:25	
	$i = 4$	50:50	
$N = 9$	$i = 1, 2, 4, 5, 7, 8$	43:33:18:5	
	$i = 3, 6$	33:33:33	
$N = 10$	$i = 1, 3, 7, 9$	39:32:20:8:1	
	$i = 2, 4, 6, 8$	36:36:14:14	
	$i = 5$	20:20:20:20:20	
$N = 11$	$i = 1, \ldots, 10$	36:30:21:11:3	
$N = 12$	$i = 1, 5, 7, 11$	33:28:21:12:5:0.6	
	$i = 2, 10$	33:25:25:8:8	
	$i = 3, 9$	28:28:28:5:5:5	
	$i = 4, 8$	25:25:25:25	
	$i = 6$	33:33:33	

[a]Shown are all configurations with low $N \leq 12$ and symmetrical input distribution. Splitting into two channels, for example, can be obtained at the ratios 100:0, 85:15, 72:28, and 50:50.

Here we present an alternative consideration and include the phases of the images.

As discussed for general M, (symmetrical) input at the center

$$x^{in} = \frac{W}{2} \tag{39}$$

of the MMI coupler of length

$$L = \frac{3L_c}{4K} \tag{40}$$

yields K self-images of equal intensities

$$r^2 = \frac{1}{K}. \tag{41}$$

Positions of the nonvanishing images j are given in Eq. (21) with Eq. (25). The illustration in Fig. 9 introduces the numbering of the nonzero outputs with indices

$$p = \frac{1}{2} + \frac{j}{4}. \tag{42}$$

Output positions are then

$$x_p^{out} = W - \frac{W}{K}\left(p - \frac{1}{2}\right), \quad \text{with } p = 1, 2, \ldots, K. \tag{43}$$

The phases of the images are calculated from Eq. (27):

$$\Phi_p = \varphi_0^* + \frac{\pi}{K}(p - 1)(K - p). \tag{44}$$

Because for many applications the relative phases are important, we have given the formula with p-dependent terms plus a constant phase φ_0^*. We have already presented this end result in Ref. 17 without derivation. Now we include the constant phase

$$\varphi_0^* = \varphi_0 + \frac{\pi}{4K}(3K^2 + 2K - 1)$$
$$= -\frac{2\pi n}{\lambda} L - \frac{\pi}{4K}(K^2 - 3K + 1), \tag{45}$$

where L is the length of the MMI coupler given in Eq. (40).

Antisymmetrical inputs at the center of the above MMI couplers produce K images also. They are positioned, however, at places in between those for symmetrical inputs. Phases for antisymmetrical inputs can be calculated in the same manner as for the symmetrical distributions.

To obtain K images we chose short devices of length $3L_c/4K$. A longer configuration of length $3L_c/2K$ exists, with odd K yielding K images of equal intensities (see Fig. 6). In contrast to the short configuration, the second one produces the reduced number of images for symmetrical and antisymmetrical images at the same positions with a phase shift included. Again, phases for these images can be calculated in the same way. To our knowledge, the latter two configurations are mentioned here for the first time. We did not investigate these in detail because the first configuration is of highest interest. Nevertheless, we have shown that our method is capable of discovering new functionalities.

C. Input at One Third: Uniform $2 \times K$ Multimode Interference Coupler

MMI couplers with symmetrical inputs at one or two thirds permit uniform power splitting into K chan-

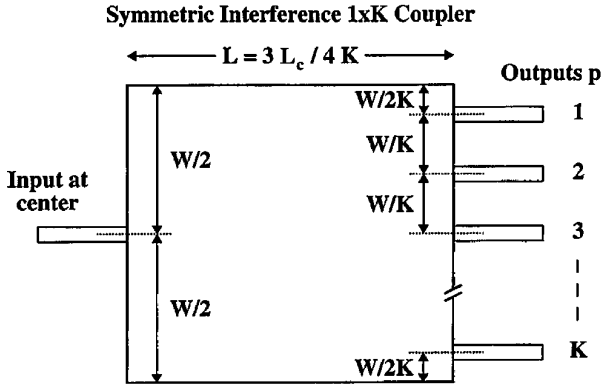

Fig. 9. Geometrical arrangement of $1 \times K$ splitter with symmetrical input at the center. K equally intense images are obtained at a device length of $L = 3L_c/4K$. Phases of the images are given in the text.

nels at a reduced length. The results of Subsection 4.C. for general M are now applied to short devices with $M = 1$. With symmetrical input at one or two thirds, modes of number 2, 5, 8, . . . are not excited because they have a node at that position. Through the use of this picture, the reduced number of images has been found for $K = 2$.[13,14] With our alternative consideration, we obtain for the first time any number K of images including their phases. We predict that antisymmetrical inputs will not build a reduced number of equally intense self-images, unlike the case with central input. Symmetrical input at

$$x^{\text{in}} = \frac{2W}{3} \tag{46}$$

of the MMI coupler of length

$$L = \frac{L_c}{K} \tag{47}$$

results in K self-images of equal intensities

$$r^2 = \frac{1}{K}. \tag{48}$$

The nonvanishing images j [see Eq. (32)] are numbered by the use of indices p:

$$\begin{aligned} j &= 6k + 2 \Rightarrow j = 3p - 1 \Rightarrow p \text{ odd}, \\ j &= 6k - 2 \Rightarrow j = 3p - 2 \Rightarrow p \text{ even}. \end{aligned} \tag{49}$$

The positions of the images $p = 1, 2, \ldots, K$ (see Fig. 10) are obtained from Eq. (30) with Eq. (49):

$$\begin{aligned} x_p{}^{\text{out}} &= W - \frac{W}{K}\left(p - \frac{1}{3}\right), \qquad p \text{ odd}, \\ x_p{}^{\text{out}} &= W - \frac{W}{K}\left(p - \frac{2}{3}\right), \qquad p \text{ even}. \end{aligned} \tag{50}$$

The phases are calculated with Eq. (33), where the addition of phase π depends on the values of $3K - j$. Because the addition of π is needed for odd $K - p$, we add $(K - p)\pi$ and obtain for the phases (after replacement of j by p and some rearrangements)

$$\begin{aligned} \Phi_p &= \varphi_0 + \frac{\pi}{12K}(8K^2 - 1) + \frac{\pi}{4K}p(2K + 2 - 3p), \\ &\qquad\qquad p \text{ odd}, \\ \Phi_p &= \varphi_0 + \frac{\pi}{12K}(8K^2 - 6K - 4) + \frac{\pi}{4K}p(2K + 4 - 3p), \\ &\qquad\qquad p \text{ even}, \end{aligned} \tag{51}$$

where we included the constant phase of Eq. (10). Splitting into p-dependent and constant terms yields:

$$\begin{aligned} \Phi_p &= \varphi_0{}^* + \frac{\pi}{4K}p(2K + 2 - 3p), \qquad p \text{ odd}, \\ \Phi_p &= \varphi_0{}^* + \frac{\pi}{4K}p(2K + 4 - 3p) - \frac{\pi}{4K}(2K + 1), \\ &\qquad\qquad p \text{ even}, \end{aligned} \tag{52}$$

with the constant phase

$$\begin{aligned} \varphi_0{}^* &= \varphi_0 + \frac{\pi}{12K}(8K^2 - 1) \\ &= -\frac{2\pi n}{\lambda}L - \frac{\pi}{12K}(K^2 - 3K + 1). \end{aligned} \tag{53}$$

Device length L is given in Eq. (47).

The above equations have been obtained for input at $2W/3$. The other input at $W/3$ can be considered by the use of symmetry arguments. Note that for odd K the output channels are not positioned at the same places for the two inputs. Because the two inputs have to be considered separately, no common output numbering is needed. For even K, however, outputs for inputs at one and two thirds are located at the same positions. Using the symmetry of the problem, we obtain for the upper input top-down output numbering and for the lower input bottom-up numbering. To use a common numbering, we explicitly give the formulas for input at

$$x^{\text{in}} = \frac{W}{3}, \tag{54}$$

with identical output numbering. We obtain this by replacing p by $K + 1 - p$. With even K, even p becomes odd. We get for the phases

$$\begin{aligned} \Phi_p &= \varphi_0{}^* + \frac{\pi}{4K}(2p - 3p^2) - \frac{\pi}{4}(K - 2), \\ &\qquad\qquad p \text{ odd}, \\ \Phi_p &= \varphi_0{}^* + \frac{\pi}{4K}(4p - 3p^2 - 1) - \frac{\pi}{4}(K - 2) + \pi, \\ &\qquad\qquad p \text{ even}. \end{aligned} \tag{55}$$

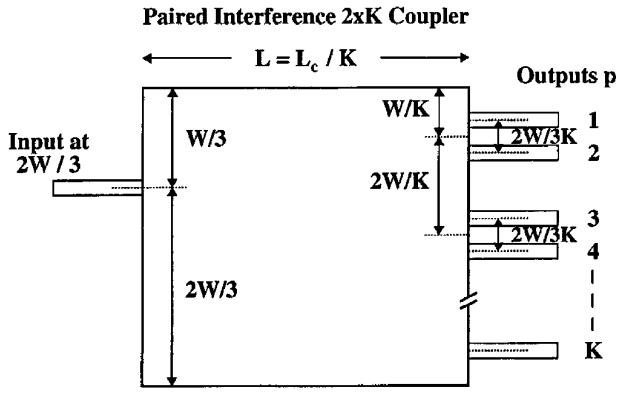

Fig. 10. Geometrical arrangement of $2 \times K$ splitter with symmetrical input at two thirds of the width. K equally intense images are obtained at a device length of $L = L_c/K$. Phases of the images are given in the text.

We have already given the relative phases of Eq. (51) in Ref. 17 for even K. Here we included the derivation and the constant phase.

D. Multimode Interference Couplers with Novel Functionalities

The overlapping-image MMI couplers build different self-images for the symmetrical and antisymmetrical parts of an arbitrary input light distribution. This can be controlled in order to have new functionalities such as mode filter, a mode splitter–combiner, and a mode converter. A simple mode filter as proposed in Fig. 11A selects the symmetrical part from an arbitrary input. The device has length $L = 3L_c/4$ and a central input. The symmetrical part is imaged to the central output (see Fig. 6), and the antisymmetrical part is imaged to the edges of the MMI coupler, which is therefore cut into two parts.

A more complex device consisting of two MMI couplers and connecting waveguides is shown in Figs. 11B and 11C. This device can be used as a mode filter for symmetrical as well as antisymmetrical distributions: From an input light distribution from the left, the symmetrical part is imaged to the central output, whereas the antisymmetrical part is imaged to the upper output. In addition, the device is a mode splitter–combiner, i.e., arbitrary input distributions are split into symmetrical and antisymmetrical parts. Finally, the proposed device is a mode converter: For strongly guided modes, the two parts of the image of antisymmetrical distributions after the first MMI coupler closely match the modes of a waveguide of half the width. Correct phase adjustment allows for constructive interference between the two parts in the second MMI coupler. The first-order mode is converted into the fundamental mode.

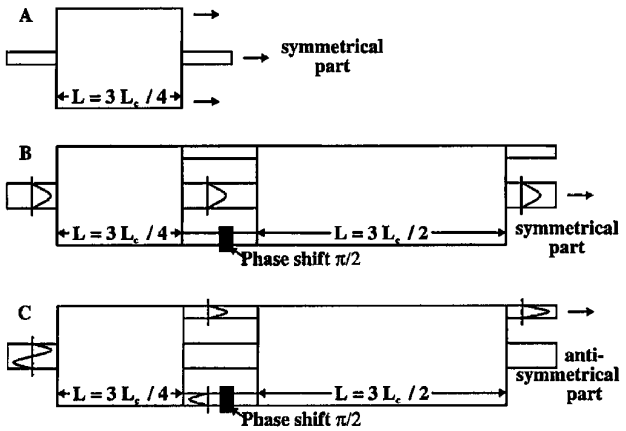

Fig. 11. Overlapping-image MMI couplers allow for new functionalities, such as a mode filter, a mode splitter–combiner, and a mode converter. A, schematic of a mode filter for symmetrical light distributions. B and C, the same device with different input distributions, showing filtering of the symmetrical and antisymmetrical part of the input light distribution, respectively. Symmetrical and antisymmetrical inputs appear at different outputs. The device is a mode splitter–combiner. The lowest antisymmetrical mode is converted into a symmetrical mode. The device is a mode converter.

E. Cosine-Square Intensity Distribution

With overlapping-image MMI couplers, different intensity distributions can be achieved. One example is power distribution into N channels following a cosine-square function. The number of periods can be selected by the input channel number. One period is obtained as follows. With symmetrical input at $x^{\text{in}} = 2W/N$ to a device of length $L = 3L_c/N$, self-images are positioned at $x_p{}^{\text{out}} = W - p2W/N$ with intensities

$$r_p{}^2 = \frac{4}{N}\cos^2\left(\frac{\pi}{2} - p\,\frac{2\pi}{N}\right), \quad \text{with } p = 1, 2, 3, \ldots, < N/2. \tag{56}$$

This is a cosine-square intensity distribution with the maximum at the central output channel and intensities diminishing toward the outer channels.

F. Specific Example of $N = 12$

This configuration includes three different cases of importance in the same device: the $1 \times K$ splitter with $K = N/4 = 3$, the $2 \times K$ splitter with $K = N/3 = 4$, and unequal power splitting. The different cases are selected by the input position. Inputs are positioned at

$$x_i^{\text{in}} = i\,\frac{W}{N} = i\,\frac{W}{12}. \tag{57}$$

Possible output locations are at

$$x_j^{\text{out}} = W - j\,\frac{W}{N} = W - j\,\frac{W}{12}, \quad \text{with } i + j \text{ even}. \tag{58}$$

A symmetrical or antisymmetrical input at the center ($i = 6$) yields $K = N/4 = 3$ images with uniform intensities of 33%. Output positions are obtained for $j = 2, 6, 10$ for symmetrical inputs and in between for antisymmetrical inputs.

A symmetrical input at one or two thirds ($i = 4, 8$) results in $K = N/3 = 4$ self-images with equal intensities of 25%. They are positioned at x_j^{out} with $j = 2, 4, 8, 10$. Symmetrical or antisymmetrical inputs to the remaining channels result in self-images with nonuniform intensities. For symmetrical input, the splitting ratios are given in Table 1.

6. Generalized Phase Diversity Relation

Properly selected input positions have led to coherently overlapping self-images. Interfering images can alternatively be realized by the simultaneous excitation of two input channels of a general $N \times N$ MMI coupler (Fig. 2). In this case, parameter a can be freely chosen. The output intensities depend on the relative phases of the inputs. For 4×4 MMI couplers, the mixed signals at the output channel are

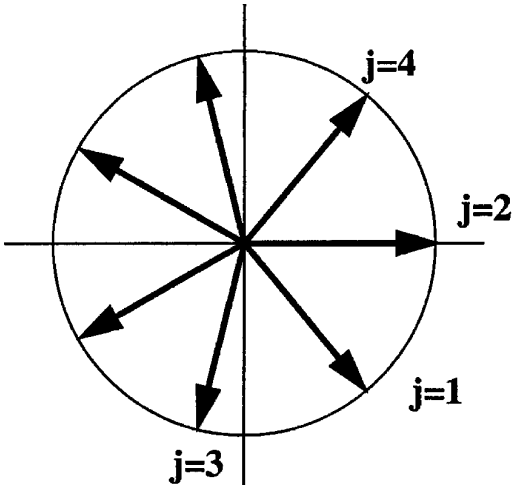

Fig. 12. Generalized phase diversity relation in $N \times N$ MMI couplers. At outputs j the signals from two inputs are mixed with phase differences varying in constant steps. The figure represents the term $2\pi A_j/N$ of Eq. (60) as a function of output number j.

in phase quadrature.[7] Here we derive a similar property for the general case of $N \times N$ MMI couplers.

Phases φ_{ij} for imaging input i to output j are given in Ref. 10. They can be reformulated as

$$\varphi_{ij} - \varphi_{2j} = \varphi_{i2} - \varphi_{22} + \frac{2\pi}{N} A_i A_j,$$

$$A_\xi = (\xi - 2)/2 \qquad \text{for } \xi \text{ even},$$

$$A_\xi = N - (\xi + 1)/2 \qquad \text{for } \xi \text{ odd}, \tag{59}$$

with $\xi = i$ or $\xi = j$. Symmetry relation $\varphi_{ij} = \varphi_{ji}$ can directly be derived from Eq. (59).

For exciting two inputs i and i' simultaneously, we obtain

$$\varphi_{ij} - \varphi_{i'j} = (\varphi_{i2} - \varphi_{i'2}) + \frac{2\pi}{N}(A_i - A_{i'})A_j. \tag{60}$$

The first term on the right-hand side is independent of output number j. For the case $(A_i - A_{i'}) \bmod N = 1$, which can be obtained with $i = 2$ and $i' = 1$, for example, signals from the two inputs are mixed at the outputs j with phase differences varying with a constant step $2\pi/N$ (Fig. 12). This characteristic is the generalized phase diversity relation for the $N \times N$ MMI couplers.

7. Conclusions

Multimode interference couplers, which produce overlapping images for light input at well-defined positions, have been introduced as a new class of devices. They allow for uniform as well as for nonuniform power splitting. Because images merge in pairs, a reduced number of self-images as compared with general $N \times N$ MMI couplers is obtained. Compact equations for image intensities, positions, and phases at arbitrary device lengths have theoretically been derived. In general, these equations lead to nonuniform intensity distributions. Among the many possibilities, imaging into two channels with ratios of 15:85 and 28:72 is shown. The theory gives all configurations for uniform intensity distribution, including the known cases of $1 \times N$ and $2 \times N$ MMI couplers. To our knowledge, their image properties have been derived for the first time. In addition, uniform splitting of antisymmetrical light distributions has been shown. Applications of MMI couplers with new functionalities such as mode filters, mode splitter–combiners, and mode converters have been proposed. Finally, a generalized phase diversity relation has been derived.

This study was done as part of the RACE-ATMOS project of the European Community and was supported by the Swiss Office for Education and Science.

References

1. O. Bryngdahl, "Image formation using self-imaging techniques," J. Opt. Soc. Am. **63,** 416–419 (1973).
2. L. B. Soldano and E. C. M. Pennings, "Optical multi-mode interference devices based on self-imaging: principles and applications," J. Lightwave Technol. **73,** 615 (1995).
3. R. van Roijen, E. C. M. Pennings, M. J. N. van Stralen, T. van Dongen, B. H. Verbeek, and J. M. M. van der Keijden, "Compact InP-based ring lasers employing multimode interference couplers and combiners," Appl. Phys. Lett. **64,** 1753–1755 (1994).
4. J. E. Zucker, K. L. Jones, T. H. Chiu, B. Tell, and K. Brown-Goebeler, "Strained quantum wells for polarization-independent electrooptic waveguide switches," J. Lightwave Technol. **10,** 1926–1930 (1992).
5. M. Bachmann, M. K. Smit, P. A. Besse, E. Gini, H. Melchior, and L. B. Soldano, "Polarization-insensitive low-voltage optical waveguide switch using InGaAsP/InP four-port Mach-Zehnder interferometer," in *Optical Fiber Conference and International Conference on Integrated Optics and Optical Fiber Communication,* Vol. 4 of 1993 OSA Technical Digest Series (Optical Society of America, Washington, D.C., 1993), pp. 32–33.
6. M. Bachmann, Ch. Nadler, P. A. Besse, and H. Melchior, "Compact polarization-insensitive multi-leg 1×4 Mach-Zehnder switch in InGaAsP/InP," in *Proceedings of the European Conference on Optical Communication* (Istituto Internationale delle Comunicazioni, Genova, Italy, 1994), pp. 519–522.
7. Th. Niemeier and R. Ulrich, "Quadrature outputs from fiber interferometer with 4×4 coupler," Opt. Lett. **11,** 677–679 (1986).
8. E. C. M. Pennings, R. J. Deri, R. Bhat, T. R. Hayes, and N. C. Andreadakis, "Ultracompact integrated all-passive optical 90° hybrid using self-imaging," in *Proceedings of the European Conference on Optical Communication* (Istituto Internationale delle Comunicazioni, Genova, Italy, 1992), pp. 461–464.
9. R. J. Deri, E. C. M. Pennings, A. Scherer, A. S. Gozdz, C. Caneau, N. C. Andreadakis, V. Shah, L. Curtis, R. J. Hawkins, J. B. D. Soole, and J. I. Song, "Ultracompact, monolithic integration of balanced, polarization diversity photodetectors for coherent lightwave receivers," Photon. Technol. Lett. **4,** 1238–1240 (1992).
10. M. Bachmann, P. A. Besse, and H. Melchior, "General self-imaging properties in $N \times N$ multimode interference couplers including phase relations," Appl. Opt. **33,** 3905–3911 (1994).
11. R. M. Jenkins, J. M. Heaton, D. R. Wight, J. T. Parker, J. C. H. Birbeck, G. W. Smith, and K. P. Hilton, "Novel $1 \times N$ and $N \times N$

integrated optical switches using self-imaging multimode GaAs/AlGaAs waveguides," Appl. Phys. Lett. **64,** 684–686 (1994).
12. C. van Dam, M. R. Amersfoort, G. M. ten Kate, F. P. G. M. van Ham, M. K. Smit, P. A. Besse, M. Bachmann, and H. Melchior, "Novel InP-based phased-array wavelength demultiplexer using a generalized MMI-MZI configuration," in *Proceedings of the European Conference on Integrated Optics* (Delft U. Press, Delft, The Netherlands, 1995), pp. 275–278.
13. E. C. M. Pennings, "Bends in optical ridge waveguides, modeling and applications," Ph.D. dissertation (Delft University of Technology, Delft, The Netherlands, 1990), ISBN 90-9003413-7.
14. L. B. Soldano, F. B. Veerman, M. K. Smit, B. H. Verbeek, A. H. Dubost, and E. C. M. Pennings, "Planar monomode optical couplers based on multimode interference effects," J. Lightwave Technol. **10,** 1843–1849 (1992).
15. R. M. Jenkins, R. W. J. Devereux, and J. M. Heaton, "Waveguide beam splitters and recombiners based on multimode propagation phenomena," Opt. Lett. **17,** 991–993 (1992).
16. A. Ferraras, F. Rodríguez, E. Gómez-Salas, J. L. de Miguel, and F. Hernández-Gil, "Useful formulas for multimode interference power splitter/combiner design," Photon. Technol. Lett. **5,** 1224–1227 (1993).
17. P. A. Besse, M. Bachmann, and H. Melchior, "Phase relations in multi-mode interference couplers and their application to generalized integrated Mach-Zehnder optical switches," in *Proceedings of the European Conference on Integrated Optics* (Ville de Neuchatel, Neuchatel, Switzerland, 1993), pp. 2.22–2.23.
18. G. J. M. Krijnen, A. Villeneuve, G. I. Stegeman, S. Aitchison, P. V. Lambeck, and H. J. W. M. Hoekstra, "Modelling of a versatile all-optical Mach-Zehnder switch," in *International Symposium on Guided-Wave Optoelectronics* (Weber Research Institute, Brooklyn, N.Y., 1994), paper VII.6.
19. M. J. N. van Stralen, R. van Roijen, E. Pennings, J. van der Heijden, T. van Dongen, and B. Verbeek, "Design and fabrication of integrated InGaAsP ring lasers with MMI-couplers," in *Proceedings of the European Conference on Integrated Optics* (Ville de Neuchatel, Neuchatel, Switzerland, 1993), pp. 2.24–2.25.
20. N. Vodjdani, F. Ratovelomanana, A. Enard, G. Glastre, D. Rondi, R. Blondeau, T. Durhuus, C. Joergensen, B. Mikkelsen, K. E. Stubkjaer, P. Pagnod, R. Baets, and G. Dobbelaere, "All optical wavelength conversion at 5 Gbit/s with monolithic integration of semiconductor optical amplifiers in a passive asymmetric Mach-Zehnder interferometer," in *Proceedings of the European Conference on Optical Communication* (Istituto Internationale delle Comunicazioni, Genova, Italy, 1994), pp. 95–98.
21. Lord Rayleigh, "On copying diffraction-gratings, and on some phenomena connected therewith," Philos. Mag. **11,** 196–205 (1881).
22. P. Latimer, "Talbot plane patterns: grating images or interference effects?," Appl. Opt. **32,** 1078–1083 (1993).
23. P. A. Besse, E. Gini, M. Bachmann, and H. Melchior, "New 1×2 multi-mode interference couplers with free selection of power splitting ratios," in *Proceedings of the European Conference on Optical Communication* ((Istituto Internationale delle Comunicazioni, Genova, Italy, 1994), pp. 669–672.